Published in final edited form as:
J Chem Eng Data. 2010 September 9; 55(9): 3598–3605. doi:10.1021/je100208e.

Anthracene + Pyrene Solid Mixtures: Eutectic and Azeotropic Character

James W. Rice*, **Jinxia Fu**, and **Eric M. Suuberg**
Brown University Division of Engineering Providence, RI USA 02912

Abstract

To better characterize the thermodynamic behavior of a binary polycyclic aromatic hydrocarbon mixture, thermochemical and vapor pressure experiments were used to examine the phase behavior of the anthracene (1) + pyrene (2) system. A solid-liquid phase diagram was mapped for the mixture. A eutectic point occurs at 404 K at $x_1 = 0.22$. A model based on eutectic formation can be used to predict the enthalpy of fusion associated with the mixture. For mixtures that contain $x_1 < 0.90$, the enthalpy of fusion is near that of pure pyrene. This and X-ray diffraction results indicate that mixtures of anthracene and pyrene have pyrene-like crystal structures and energetics until the composition nears that of pure anthracene. Solid-vapor equilibrium studies show that mixtures of anthracene and pyrene form solid azeotropes at x_1 of 0.03 and 0.14. Additionally, mixtures at $x_1 = 0.99$ sublime at the vapor pressure of pure anthracene, suggesting that anthracene behavior is not significantly influenced by $x_2 = 0.01$ in the crystal structure.

Introduction

Polycyclic aromatic hydrocarbons (PAH) are normally found in mixtures of many similarly structured compounds. The goal of the present research is to better understand PAH mixture thermodynamics by studying the phase behavior of a binary anthracene (1) + pyrene (2) system. Anthracene and pyrene consist of three and four fused aromatic rings respectively. They are common PAH and are common components of PAH mixtures.

Similar studies have been conducted on binary, organic component mixtures and these principally report the temperatures and enthalpies of solid to liquid phase transitions, often involving one or two eutectic points. Table 1 summarizes melting temperatures of reported binary, aromatic-containing mixtures that form eutectics. Tables S1, S2, S3 are provided as supporting information to further summarize the fusion and interaction energies of other, recently studied binary aromatic-containing mixtures.[8-11] It is worth noting that other groups have studied the phase behavior of anthracene + pyrene mixtures, reporting the formation of a eutectic.[3,4] However, these were only melting temperature studies that did not provide the necessary data to fully characterize the mixture thermodynamics. Hence, in addition to melting temperature analysis, the present study focused on enthalpies of fusion, microstructure, and vapor pressure of this complicated, binary PAH system. In addition to fusion behavior, many of the results presented here will address the sublimation behavior of the system given that the anthracene + pyrene solid-vapor system is not yet well understood or reported on in the literature.

*401-863-2775 (p) 401-863-9120 (f) James_Rice@Brown.edu.

Supporting Information Available A review of previously studied eutectic, binary, organic component mixtures is contained in Tables S1, S2, S3. Additional X-ray and vapor pressure results for mixtures of anthracene (1) + pyrene (2) are provided. This information is available free of charge via the Internet at http://pubs.acs.org/.

Experimental

Materials

Anthracene (CAS Reg. No. 120-12-7, with mass fraction purity >0.99) and pyrene (CAS Reg. No. 129-00-0, with mass fraction purity >0.97) were obtained from Aldrich and TCI America respectively. Purity was verified by GC-MS analysis. The anthracene contained trace levels of phenanthrene. Analysis of pyrene showed one impurity with ions at mass-to-charge ratios (*m/z*) of 208 and 104. This spectrum could not be identified and further experiments verified that it does not represent anthraquinone (which would not split to an *m/z* of 104, but does have a molar mass of 208 $g \cdot mol^{-1}$). The 208 to 104 *m/z* split is characteristic of a PAH or long-chain organic that is able to break in half upon ionization.

In addition, the melting temperature of each pure compound, $T_{fus,1}$ = (490 ± 1) K and $T_{fus,2}$ = (424 ± 1) K, was measured and compared favorably to the literature values.[3, 4] The details of the melting temperature analysis are discussed in a later section.

Mixture Preparation

Mixtures of anthracene and pyrene were prepared using a melt and quench-cool technique. The desired quantities of anthracene (1) + pyrene (2) were measured to ± 0.01 mg and sealed within a brass vessel. The vessel was then heated to (498 ± 5) K and agitated, ensuring that both components melted and mixed in a liquid state. After a period of 5 min, the vessel was removed from the heat source and immediately immersed in liquid nitrogen, which provided cooling at an estimated (70 to 80) $K \cdot s^{-1}$ for the first 4 sec. The preparation technique intended to preserve the disorder of the well-mixed liquid during crystallization. This heating and quench-cool procedure was repeated 4 additional times before the mixture crystals were removed from the preparation vessel and placed in glass storage vials. Uniformity of the samples was confirmed by visual examination. As it turned out, the results presented below were largely insensitive to the details of the preparation of the mixture (see below).

Melting Temperature and Enthalpy of Fusion

Melting temperatures and enthalpies of fusion ($\Delta_{fus}H$) of mixtures and pure samples were measured using a Thermo Scientific melting temperature analyzer and DuPont differential scanning calorimeter (DSC). In the latter case, hermetically sealed DSC pans were filled with (1 to 3) mg of sample and scanned in both heating and cooling modes. The rates of heating and cooling were 10 $K \cdot min^{-1}$ and 2.5 $K \cdot min^{-1}$ respectively. This procedure produces conveniently integrable peaks, increasing the accuracy of the enthalpy of fusion calculation. However, the values of enthalpy and transition temperatures were generally insensitive to changes in heating and cooling rate in the range of (2.5 to 20) $K \cdot min^{-1}$. A melting temperature analyzer was used to visually observe and obtain higher resolution melting temperature measurements. These generally agreed with the DSC in that the melting temperatures from each instrument differed by no more than 4 K, though naturally what is reported from the DSC is a temperature from an endothermic event stretching over several degrees, and hence, these values are less precise than classic melting temperature determination.

Melting behavior was tracked using the melting temperature analyzer to ± 1 K. In following the thaw-melt method,[1] (1 to 2) mg of each sample was placed inside a glass capillary tube and heated at (1 ± 0.5) $K \cdot min^{-1}$. The thaw temperature is the temperature at which the first droplet of liquid appears in the capillary tube. The liquidus temperature is the maximum temperature at which both solid-crystals and liquid are observed to coexist in the system. Hence, the liquidus temperature is reached when the last crystal melts in the capillary tube.

The experimentally measured enthalpies of fusion, thaw temperatures, and liquidus temperatures have been used to build a phase diagram for the anthracene + pyrene solid-liquid system.

Vapor Pressure

The Knudsen effusion technique was used to measure the vapor pressures (P) of solid anthracene + pyrene mixtures and pure components. This technique allows for vapor pressure measurement of low volatility compounds. Traditional vapor pressure techniques measure pressure directly and would require unacceptably high experimental temperatures that could degrade both anthracene and pyrene. The Knudsen effusion technique measures sample mass loss from a confining cell through a small orifice and relates it to vapor pressure by

$$P=\frac{m}{AW}\sqrt{\frac{2\pi RT}{M}} \quad [1]$$

where m is the mass loss rate, A is the orifice area, R is the universal gas constant, T is the sample temperature, and M is the molecular weight. The Clausing correction factor W, gives the probability that an effusing molecule will escape from the cell. It is determined by experimental calibration or calculated empirically by

$$W=\frac{1}{1+{}^{3l}/_{8r}} \quad [2]$$

where l is the orifice effusion length and r is the orifice radius. Values of W for this study approach unity, ranging between 0.96 and 0.98. Vapor pressure experiments must satisfy fundamental effusion theory, which stipulates that vapor molecules escape a confining cell through orifice passages that are much smaller than their molecular mean free path. A detailed explanation of the Knudsen effusion theory and its implementation in this laboratory can be found elsewhere.[13, 14]

Samples of anthracene (1) + pyrene (2) were placed inside effusion cells prepared from steel shim stock. The cells were sealed except for a single, circular orifice of diameter (0.60 ± 0.01) mm and placed on the arm of a continually recording microbalance contained in a high vacuum chamber. The pressure inside the chamber was reduced to 10^{-4} Pa to achieve the required condition of negligible backpressure outside the orifice. A calibrated, type-K thermocouple was used to measure cell temperature to ± 0.1 K and to verify thermal equilibrium in the system. At equilibrium, the pressure inside the cell is the vapor pressure of the sample and the subliming species will leak from the cell through the small orifice. The leak rate is measured and correlated to vapor pressure with eq 1. The relative instrument uncertainty within the experimental temperature range is $\delta P/P = 0.045$. In the case of a mixture, there is obviously a question of what molecular weight must be used for M. In this work, the decision was made to use a weighted average of pure component molecular weights. Because the value of molecular weight appears as the square root, there is not particularly great sensitivity to this value. For example, use of the above, assumed value would result in a maximum difference of 2.6 % in measured vapor pressure, if we take an extreme composition at $x_1 = 0.90$ at an experimental temperature of 338 K. Such a small difference is seen to be within the overall uncertainties.

With respect to the values of measured vapor pressures for mixtures, it is important to recognize that what is being examined is a solid sublimation system. The temperatures are

always so low that there will be no formation of a liquid phase. This is important to keep in mind, insofar as the behavior of this system is inherently different than that of a liquid mixture system. If the fundamental condition of thermodynamic equilibrium in the sample cell is fulfilled (as must be considered reasonable), then it is important to recognize that equilibrium must be satisfied for all phases that might be present. What this means is that if a molecular component of a particular solid mixture were to have a sublimation pressure above the sublimation pressure of that pure component, a new pure component phase would be nucleated, even if it were not present in the quench-cooled mixture. In other words, the vapor pressure of the system would be bounded on the upper side by the sum of pure component vapor pressures. This is different than in liquid systems, in which mixing would be more favored and the same sort of phase separation would not necessarily be possible.

Other Sample Characterizations

The crystal structures of anthracene, pyrene, and their mixtures were qualitatively investigated using powder X-ray diffraction (XRD). Samples were reduced to a fine powder and dusted onto glass slides that were coated with a thin petroleum film. A Siemens X-ray diffractometer (model D5000) was used to measure the diffraction patterns of each sample between (10 and 60)°.

Gas chromatography-mass spectrometry (GC-MS) was used to determine the composition of mixtures before, during, and after vapor pressure experiments. Analytes were dissolved in dichloromethane to an approximate concentration of 100 $\mu g \cdot ml^{-1}$ and analyzed by a calibrated Varian combined gas chromatograph (model CP3800) and mass spectrometer (model Saturn 2200). The Varian analytical procedure for EPA Method 8270C was followed.[15]

Results and Discussion

Phase Diagram and Enthalpy of Fusion

Enthalpies of fusion for all samples were measured using temperature-controlled differential scanning calorimetry. Results from typical DSC scans are given in Figure 1. All four scans were conducted in heating-mode between 298 K and 523 K at 10 $K \cdot min^{-1}$. The DSC results here show heat input ($\varphi/W \cdot g^{-1}$) as the system is heated. Peaks in the DSC scan reveal phase changes. The four scans in Figure 1 have peaks that represent endothermic, solid to liquid phase transitions. Peaks can be integrated to determine the enthalpy of fusion of the sample with a relative uncertainty of $\delta\Delta_{fus}H/\Delta_{fus}H = 0.07$. Pure anthracene and pyrene melt at 490 K with $\Delta_{fus}H = (156 \pm 11.9)\ J \cdot g^{-1}$ and 424 K with $\Delta_{fus}H = (80 \pm 5.6)\ J \cdot g^{-1}$ respectively. These results are in fair agreement with those of Domalski and Hearing, who report that pure anthracene and pyrene melt at 489 K with $\Delta_{fus}H = 164.8\ J \cdot g^{-1}$ and 423 K with $\Delta_{fus}H = 85.8\ J \cdot g^{-1}$ respectively.[16]

Mixture compositions are given in terms of x_1 as it is understood that $x_1 + x_2 = 1$. The DSC results indicate that anthracene (1) + pyrene (2) quench-cooled mixtures in the indicated composition range undergo a phase transition at 404 K, well before either of the pure phases melts. This indicates the existence of a eutectic mixture. In some cases, such as the one shown for a mixture at $x_1 = 0.90$, there appear to be two phase transitions as the sample is heated.

It is important to recall that the results are all for quench-cooled samples. If similar DSC experiments are performed on physical anthracene (1) + pyrene (2) mixtures, the measured values of melting temperature and fusion enthalpy match those of the quench-cooled samples. This suggests that vapors interdiffuse in the vapor-solid system and that a

thermodynamically favored eutectic exists for this anthracene + pyrene system, irrespective of initial preparation.

It is worth noting with regard to the results of Figure 1 that all evidence of a pyrene solid phase disappears in the presence of the lower temperature eutectic phase peak, irrespective of the magnitude of that latter peak. In other words, it appears as though pure pyrene is not a stable phase in such mixture systems. Figure 2 shows the full heating, cooling, and reheating scan of an equimolar anthracene + pyrene mixture. As with the mixture at $x_1 = 0.90$, the equimolar mixture at $x_1 = 0.50$ appears to undergo two endothermic phase transitions upon heating. Then cooling at a rate of 2.5 $K \cdot min^{-1}$ induces crystallization at 426 K of what is most probably an inhomogeneous phase that has limited solubility in the eutectic. This is followed by crystallization of the eutectic phase itself at 390 K. Each of these phase transitions represents the crystallization of a subcooled liquid. When reheated, the phase transitions and associated temperatures match those of the initial heating sequence (Figure 2). Additionally, when nucleation of the eutectic phase is prevented by cooling to only 398 K, the eutectic melting peak is no longer present in the reheating step (not shown). These results indicate that the two exothermic transition peaks definitively correspond to those of the two endothermic phase transitions.

In order to more completely explore phase behavior, it was necessary to use a melting temperature analyzer. Although the DSC measures the energy of a phase transition, it is not possible to visually observe the processes. Melting temperatures were measured for all pure components and mixtures and are given in Table 2. The melting temperatures were measured in heating mode at (1 ± 0.5) $K \cdot min^{-1}$. This relatively slow rate allows for more precise measurement of melting temperatures. The results show that solid, quench-cooled anthracene (1) + pyrene (2) mixtures have a eutectic point of (404 ± 1) K at $x_1 = (0.22 \pm 2 \cdot 10^{-4})$. For all other compositions, only a portion of the crystals melts at the eutectic temperature. Consequently, both solid and liquid coexist until the liquidus temperature is reached. Thus, Figure 3 represents a phase diagram for the anthracene (1) + pyrene (2) system in which only solid phases exist below the thaw curve and only a liquid phase exists above the liquidus curve. The areas between these curves show the equilibrium coexistence of both solid and liquid phases. The point at which the liquidus curve meets the thaw temperature is the anthracene + pyrene eutectic point. Similar results have been previously reported by both V. M. Kravchenko[17] and Ryszard Szczepanik3 who report a eutectic point of 403.15 K and 404.6 K at $x_1 = 0.209$ and 0.221 respectively.

In addition to the melting temperatures, the results from the thermal analyses are given in Table 2 and shown in Figure 3 . The $\Delta_{fus}H$ observed at the eutectic temperature of 404 K characterizes the necessary heat input for the initial melting to occur. The total $\Delta_{fus}H$ is a summation of both endothermic phase transition peaks observed in the DSC scan. It is worth noting that the total $\Delta_{fus}H$ is very similar to that of pure pyrene over a wide range of compositions and that the $\Delta_{fus}H$ for both pure pyrene and the eutectic mixture are very similar. What this means is that when the mixture contains only a modest amount of anthracene, energetically it behaves quite similarly to pure pyrene, and this persists until the mixture is nearly pure anthracene. There is a slight increase in fusion enthalpy when the mixtures are enriched in anthracene beyond the eutectic composition, but the shift is only modest as compared with the increase of fusion enthalpy to that of pure anthracene. This indicates that the ability of anthracene to reach a lower energy crystalline configuration is significantly impeded by the presence of relatively small amounts of pyrene.

In Figure 3, the data for $\Delta_{fus}H$ at the eutectic temperature clearly establishes that the eutectic is a thermodynamically preferred phase, whose formation is limited by the system stoichiometry. At low concentrations of anthracene, eutectic formation is limited by the

availability of anthracene. Since the actual eutectic composition occurs near $x_1 = 0.22$, at low anthracene concentrations, addition of N_1 moles anthracene produces ($N_1 + (78/22) \cdot N_1 = 4.55 \cdot N_1$) moles of eutectic. This means that as an approximation for small additions of anthracene,

$$\frac{d\Delta H_{\text{eutectic peak}}}{dN_1} = 4.55 \cdot \Delta \bar{H}_e \quad [3]$$

in which the $\Delta \bar{H}_e$ represents the molar enthalpy of fusion of the pure eutectic phase. If the addition of anthracene is done while keeping the total moles in the system roughly constant, then since $d(N_1/N_{tot}) = dx_1$ it is possible to see that

$$\frac{d\Delta H_{\text{eutectic peak}}}{dx_1} = 4.55 \cdot \Delta H_{e,max} \quad [4]$$

where $\Delta H_{e,max}$ is now the maximum enthalpy of fusion at the eutectic point. Integration gives as a result (for the relevant range of anthracene-limited eutectic formation)

$$\Delta H_{\text{eutectic peak}} = 4.55 \cdot 90\ \text{J} \cdot \text{g}^{-1} \cdot x_1 = 410 \cdot x_1\ \text{J} \cdot \text{g}^{-1} \quad [5]$$

This is valid only for $x_1 < 0.22$. So for example at $x_1 = 0.10$, the predicted enthalpy for the 404 K peak is 41 $\text{J} \cdot \text{g}^{-1}$, whereas the measured value is just slightly greater than this.

Beyond the eutectic composition, $x_1 > 0.22$, the concentration of pyrene is assumed to limit the ability to form the eutectic phase. Again, for the eutectic, it is true that ($x_{1,e}/x_{2,e} = 0.22$ 0.78 = 0.282). The fraction of moles involved in forming the eutectic can be expressed as ($x_e = x_{1,e} + x_{2,e}$), but since pyrene is assumed to be the limiting component, it is possible to say that ($x_2 = x_{2,e}$), i.e., all of the pyrene is in the eutectic phase. It is true that ($x_1 + x_2 = 1$), which means

$$x_e = x_{1,e} + (1 - x_1) = 0.282 \cdot x_{2,e} + (1 - x_1) = 1.282 \cdot (1 - x_1) \quad [6]$$

This in turn means that for $x_1 > 0.22$

$$\frac{d\Delta H_{\text{eutectic peak}}}{dx_1} = -1.282 \cdot \Delta H_{e,max} \quad [7]$$

Upon integration, this yields

$$\Delta H_{\text{eutectic peak}} = 90\ \text{J} \cdot \text{g}^{-1} - 1.282 \cdot 90\ \text{J} \cdot \text{g}^{-1} \cdot (x_1 - 0.22) = 90\ \text{J} \cdot \text{g}^{-1} - 115.\ (x_1 - 0.22)\ \text{J} \cdot \text{g}^{-1} \quad [8]$$

So for example, at $x_1 = 0.50$, the enthalpy of fusion at 404 K is predicted to be about 58 $\text{J} \cdot \text{g}^{-1}$. This is in reasonable agreement with the observed value.

The agreement between the values obtained from this simple modeling of system behavior and experiment are shown in Figure 3 and strongly support the conclusion that formation of a eutectic phase at $x_1 = 0.22$ is thermodynamically favored. What this means is that the

enthalpy of fusion per gram of the non-eutectic phase is increasing proportionally with anthracene fraction, since overall, the enthalpy of fusion of the whole mixture does not vary much with composition. The enthalpy of fusion of the non-eutectic anthracene-rich phase is not the same as that of pure anthracene, meaning that there must be some contribution of pyrene to this phase until the mixture approaches truly pure anthracene.

X-Ray Diffraction

Powder X-ray diffraction studies were conducted to study the crystal structures of anthracene (1) + pyrene (2) mixtures in comparison to those of the pure components. The results are qualitative. The peak intensity from one spectrum to another has no significance and was related only to the quantity of sample used (mixtures were used more sparingly).

Peak positions from the mixture results can be compared to those of the pure component X-ray diffraction patterns. Figure 4 shows that the crystal structure of the eutectic mixture is similar to that of pyrene because peaks at (10.6, 11.6, 14.9, 16.3, 18.2, 23.3, 24.7 and 28.0) ° are all retained in the mixture diffraction pattern. This is consistent with the DSC result that implies that the $\Delta_{fus}H$ of the eutectic is very close to that of pure pyrene. This indicates that the crystal structures of the eutectic mixture and pure pyrene are similar. Likewise, Figure 4 shows that the crystal structure of a mixture at $x_1 = 0.90$ is comparable to that of pure anthracene. This suggests that the crystal structure of anthracene is approached at low levels of pyrene.

Figure S1, provided as supporting information, is an enlargement of the X-ray pattern from Figure 4 between (10 and 12) °. When reviewed at this magnification, it is possible to see the minor differences in the peaks for pyrene and the eutectic. In this case, the peak from the eutectic mixture at 10.6 ° has lost the doublet from the pure pyrene peak. Additionally, the peaks near 11.6 ° do not align perfectly. The eutectic mixture retains much of the crystal structure of pure pyrene, indicating that the eutectic composition is a pyrene-like mixture that does not completely preserve the pure component characteristics. Again, this is consistent with the results of the thermal analysis.

Vapor Pressure

Knudsen effusion experiments were conducted by measuring the vapor pressure of various initial quench-cooled mixtures and pure components. The measured vapor pressure of pure anthracene $\ln P_1$ /Pa = 32.211–11683·T /K^{-1} (300 to 373) K, and pyrene $\ln P_2$ /Pa = 31.735 – 11679·T /K^{-1} (315 to 378) K, compare favorably to literature values.[18] Based on the notion that anthracene and pyrene were individual organic compounds, it was originally hypothesized that mixtures of the two components would behave ideally and sublime according to a weighted average of pure component vapor pressures, i.e., Raoult's law would be followed. Figure 5 shows that this did not hold true. Instead of approaching the ideal mixture values, the vapor pressures of the anthracene (1) + pyrene (2) mixtures behaved as a sum of the two pure species vapor pressures. Again, this summation represents the maximum possible pressure in the effusion cell because the vapor pressure cannot exceed that of the pure, equilibrated species. These data could be interpreted as indicating that mixtures of anthracene and pyrene are phase-separated systems in which the pure species do not interact. However, the aforementioned phase diagram and X-ray data show that the species are interacting in a complicated, non-ideal way.

Vapor pressure measurements were continuously performed on a sample of known initial composition. These experiments required that the composition of the mixture be known throughout the sequence. Thus, samples were occasionally removed from the effusion cells, dissolved in dichloromethane, and analyzed by GC-MS. Reported mole fractions are

accurate to ± 0.01. Figure 6 shows the results of two experiments that examined vapor pressure as a function of mass loss of an initially eutectic mixture. Both experiments initially tracked vapor pressure at 318.2 K to the point at which the vapor pressure stabilized. It needs to be kept in mind that upon vaporization, unless both components vaporize at exactly the same rate, composition, and with that, vapor pressure, will continuously change. With reference to Figure 5, it is seen that anthracene is the more volatile pure component (despite its higher melting temperature compared with pyrene). As anthracene is then preferentially lost in the experiment of Figure 6, the vapor pressure would drop, unless the two components behave as separate pure phases. The decreasing vapor pressure shown in Figure 6 establishes that for the purposes of vapor pressure, there is interaction between components. Interestingly, a subsequent, stable vapor pressure was then achieved after loss of about 13 % by mass of the initial mixture. The overlapping vapor pressure data in the low temperature (318.2 K) region of Figure 6 represent two separate samples and demonstrate the degree of reproducibility of this experimental method.

At this point, the temperature was increased to 333.2 K and 338.2 K for the remainder of the experiments of Figure 6. As a result of the increase in temperature, measured vapor pressure increases, as expected. The dashed and dotted lines of Figure 6 show theoretical maximum vapor pressures that would exist for independent anthracene (1) and pyrene (2) phases.

GC-MS analysis showed that the mole fraction of anthracene in the solid was reduced from an initial value of $x_1 = 0.22$ to $x_1 = 0.14$ during the transient at 318.2 K. Once this stable composition was reached, both the vapor pressure and the composition remained unchanged for the remainder of the experiment. This indicates that mixtures of anthracene and pyrene form a solid-azeotrope at $x_1 = 0.14$. It is important to bear in mind the distinction between the eutectic mixture and the azeotrope. The eutectic mixture exhibits a minimum melting temperature at $x_1 = 0.22$. The azeotrope is a constant subliming mixture at $x_1 = 0.14$. There is no particular reason that the eutectic and azeotrope should occur at the same composition.

It is now possible to extract the data from Figure 6 to characterize the behavior of the azeotrope as a function of temperature (Figure 7). The maximum possible vapor pressure and Raoult's law prediction for a mixture at $x_1 = 0.14$ have been plotted along with the measured azeotrope data. Although the azeotrope happens to give a vapor pressure close to the Raoult's law value for that mixture composition, the observed behavior does not represent ideal thermodynamic mixture behavior. If the system were behaving ideally, the composition of the mixture would change throughout the experiment causing both the experimental vapor pressure and reference curves to shift accordingly. This does not occur with the azeotrope, which sublimes at constant composition.

The results for the case of an anthracene-rich mixture initially at $x_1 = 0.90$, is shown in Figure 8. The mixture also forms a solid azeotrope at $x_1 = 0.99$. This suggests the existence of an inhomogeneous mixture that must partially sublime before the solid azeotrope is reached. The vapor pressure measurements shown in Figure 8 were taken after the azeotrope concentration was achieved. The vapor pressure of the azeotrope at $x_1 = 0.99$ is close to that of pure anthracene, suggesting that the vapor pressure is insensitive to the existence of $x_2 = 0.01$ in the crystal structure. This is consistent with the X-ray patterns (Figure 4) and the phase diagram (Figure 3) showing that the anthracene-rich mixture has a crystal structure, liquidus temperature, and enthalpy of fusion approaching that of pure anthracene. In other words, the behavior of the anthracene (1) + pyrene (2) system approaches that of pure anthracene when the pyrene impurity level reaches $x_2 = 0.01$. To call this an azeotrope such as that at $x_1 = 0.14$ is perhaps misleading. In fact, it is suggested that instead, this low a level of pyrene impurity can be retained in the anthracene crystallographic structure without any significant impact on measured thermodynamic properties.

The results for the case of a pyrene-rich mixture, initially at $x_1 = 0.10$, are given in Figure 9. The mixture forms a solid azeotrope at $x_1 = 0.03$. As with the eutectic composition and anthracene-rich mixtures, this final mixture only reaches a stable vapor pressure when the azeotrope concentration is obtained. This again implies the existence of an inhomogeneous mixture that gradually gives way to the azeotrope behavior. The reference curves show that the pyrene-rich azeotrope at $x_1 = 0.03$ has a unique vapor pressure close to that of the azeotrope at $x_1 = 0.14$. This result suggests that the anthracene (1) + pyrene (2) system is capable of forming multiple azeotropes. Although binary polyazeotropy is rare, it has been reported in the literature.[19, 20] This, then, is in sharp contrast to the behavior of the anthracene-rich mixture, in which pure phase behavior was approached. Here, sublimation of the mixture occurs at constant composition, significantly removed from pure pyrene behavior, for substantial extents of mass loss. The measured vapor pressures for the three solid azeotropes are tabulated and given in Table 3. It is interesting to note that the commercial supply impurities of both anthracene and pyrene were at the respective azeotrope type limits.

Conclusions

The anthracene (1) + pyrene (2) mixture system is complicated and non-ideal. The solid-liquid equilibrium study shows that mixtures of anthracene and pyrene have a minimum melting temperature, i.e., eutectic point, of 404 K at $x_1 = 0.22$. Additionally, for a wide range of composition, the crystal structure and energetics of the anthracene + pyrene mixtures are comparable to those of pyrene. The eutectic behavior is a solid-liquid equilibrium phenomenon and should not be confused with the azeotropy observed at solid-vapor equilibrium. Mixtures of anthracene and pyrene exhibit two pyrene-rich, stable azeotropes. In contrast, at high anthracene compositions, the vapor pressure above the solid equilibrates to that of pure anthracene, indicating that anthracene can accommodate low levels of pyrene in its crystal structure. Future work will aim to characterize other binary and multicomponent mixtures of polycyclic aromatic compounds.

Supplementary Material

Refer to Web version on PubMed Central for supplementary material.

Acknowledgments

This publication was made possible by **Grant Number P42 ES013660** from the National Institute of Environmental Health Sciences (NIEHS), NIH and the contents are solely the responsibility of the authors and do not necessarily represent the official views of the NIEHS, NIH.

References

(1). Rastogi RP, Rama Varma KT. Solid–Liquid Equilibria in Solutions of Non-Electrolytes. J. Chem. Soc 1956:2097–2101.

(2). Rastogi RP, Bassi PS. Mechanism of Eutectic Crystallization. J. Phys. Chem 1964;68:2398–2406.

(3). Szczepanik R, Skalmowski W. Effects of crystal growth and volatilization of tar components on the aging of prepared tar. III. Solid-liquid phase relationship of the components of raw coal tar and prepared road tar. Bitumen, Teere, Asphalte, Peche 1963;14:506,508–512,514.

(4). Szczepanik R. Two- and multicomponent, solid-liquid systems formed by aromatic hydrocarbons, anthraquinone, and coal-tar fractions. Chem. Stosowana Ser. A 1963;7:621–660.

(5). Singh NB, Giri DP, Singh NP. Solid-Liquid Equilibria for p-Dichlorobenzene + p-Dibromobenzene and p-Dibromobenzene + Resorcinol. J. Chem. Eng. Data 1999;44:605–607.

(6). Singh NB, Das SS, Singh NP, Agrawal T. Computer simulation, thermodynamic and microstructural studies of benzamide-benzoic acid eutectic system. J. Cryst. Growth 2008;310:2878–2884.

(7). Das SS, Singh NP, Agrawal T, Gupta P, Tiwari SN, Singh NB. Studies of Solidification Behavior and Molecular Interaction in Benzoic Acid-o-Chloro Benzoic Acid Eutectic System. Mol. Cryst. Liq. Cryst 2009;501:107–124.

(8). Rai RN, Varma KBR. Phase diagram and dielectric studies of binary organic materials. Mater. Lett 2000;44:284–293.

(9). Singh NB, Srivastava MA, Singh NP. Solid-Liquid Equilibrium for 2,4-Dinitrophenol + Naphthalene. J. Chem. Eng. Data 2001;46:47–50.

(10). Singh NB, Srivastava A, Singh NP, Gupta A. Molecular Interaction between Naphthalene and 2,4-Dinitrophenol in Solid State. Mol. Cryst. Liq. Cryst 2007;474:43–54.

(11). Gupta RK, Singh RA. Thermochemical and microstructural studies on binary organic eutectics and complexes. J. Cryst. Growth 2004;267:340–347.

(12). Gupta RK, Singh SK, Singh RA. Some physiochemical studies on organic eutectics. J. Cryst. Growth 2007;300:415–420.

(13). Knudsen, M. The Kinetic Theory of Gasses. Methuen & Co., LTD; London: 1934.

(14). Oja V, Suuberg EM. Development of a Nonisothermal Knudsen Effusion Method and Application to PAH and Cellulose Tar Vapor Pressure Measurement. Anal. Chem 1997;69:4619–4626.

(15). Varian Inc. Semivolatile Organic Compounds by Gas Chromatography/Mass Spectrometry (GC/MS). Enironmental Applications Manual 2001-2004:1–29.

(16). Domalski ES, Hearing ED. Heat Capacities and Entropies of Organic Compounds in the Condensed Phase. Vol III. J. Phys. Chem. Ref. Data 1996;25:1–525.

(17). Kravchenko VM. Equilibrium of the condensation phases of 4-ring hydrocarbons with 1-, 2-, and 3-ring hydrocarbons. Pyrene systems. Ukrains'kii Khemichnii Zhurnal 1953;19:484–490.

(18). Goldfarb JL, Suuberg EM. Vapor Pressures and Enthalpies of Sublimation of Ten Polycyclic Aromatic Hydrocarbons Determined via the Knudsen Effusion Method. J. Chem. Eng. Data 2008;53:670–676.

(19). Christensen SP, Olson JD. Phase Equilibria and Multiple Azeotropy of the acetic Acid-Isobutyl Acetate System. Fluid Phase Equilib 1992;79:187–199.

(20). Aucejo A, Loras S, Munoz R, Wisniak J, Segura H. Phase Equilibria and Multiple Azeotropy in the Associating System Methanol + Diethylamine. J. Chem. Eng. Data 1997;42:1201–1207.

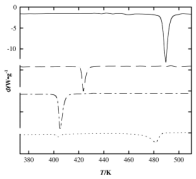

Figure 1.
Differential scanning calorimetry results of pure components and mixtures: _, pure (1); _ _ _, pure (2); _._._, mixture at $x_1 = 0.22$; …, mixture at $x_1 = 0.90$.

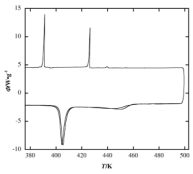

Figure 2.
Differential scanning calorimetry of an equimolar anthracene (1) + pyrene (2) mixture.

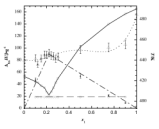

Figure 3.

Phase diagram and $\Delta_{fus}H$ of the anthracene (1) + pyrene (2) system: - ○ -, thaw curve; -□-, liquidus curve; ▲, $\Delta_{fus}H_{eutectic\ peak}$; _.._.._, estimated $\Delta_{fus}H_{eutectic\ peak}$ from eq 5 and 8; ..△.., $\Delta_{fus}H_{tot}$, with error bars representing uncertainty.

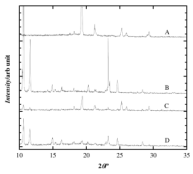

Figure 4.
X-ray diffraction patters of pure components and mixtures: A, pure (1); B, pure (2); C, anthracene-rich mixture at $x_1 = 0.90$; D, eutectic mixture $x_1 = 0.22$.

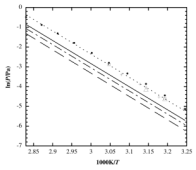

Figure 5.
Vapor pressure measurements of anthracene (1) + pyrene (2) mixtures with varied composition: _, pure (1); _ _ _, pure (2); _._._, equimolar Raoult's law prediction; …, P_{max}; ●, $P_{(1)+(2)}$ at $x_1 = 0.50$; △, $P_{(1)+(2)}$ at $x_1 = 0.10$; +, $P_{(1)+(2)}$ at $x_1 = 0.22$; □, $P_{(1)+(2)}$ at $x_1 = 0.75$.

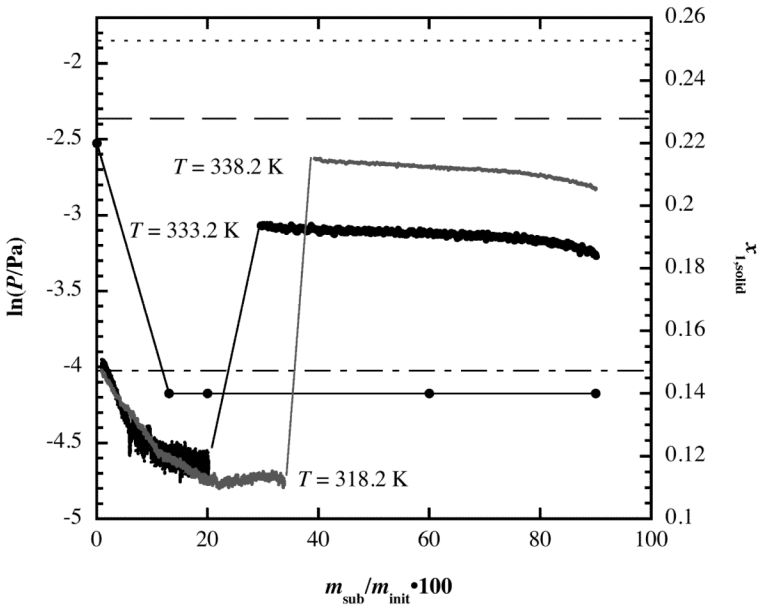

Figure 6.

Vapor pressure and composition of a eutectic anthracene (1) + pyrene (2) mixture versus sample mass loss: __, $P_{measured}$; …, $P_{max,\ 338.2\ K}$; _ _ _, $P_{max,\ 333.2\ K}$; _.._.._, P_{max}, 318.2 K; _●_, measured x_1 of solid mixture.

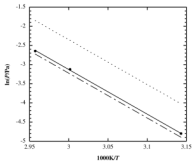

Figure 7.

Vapor pressure of the solid azeotrope at $x_1 = 0.14$: -●-, $P_{measured}$; …, P_{max}; _.._.._, Raoult's law prediction for $x_1 = 0.14$.

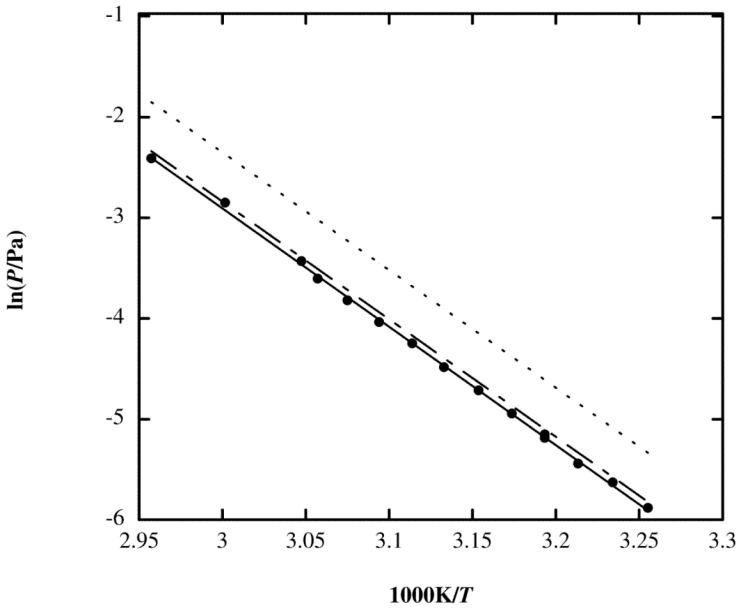

Figure 8.
Vapor pressure of the solid azeotrope at $x_1 = 0.99$: _●_, $P_{measured}$; …, P_{max}; _.._.._, P_1.

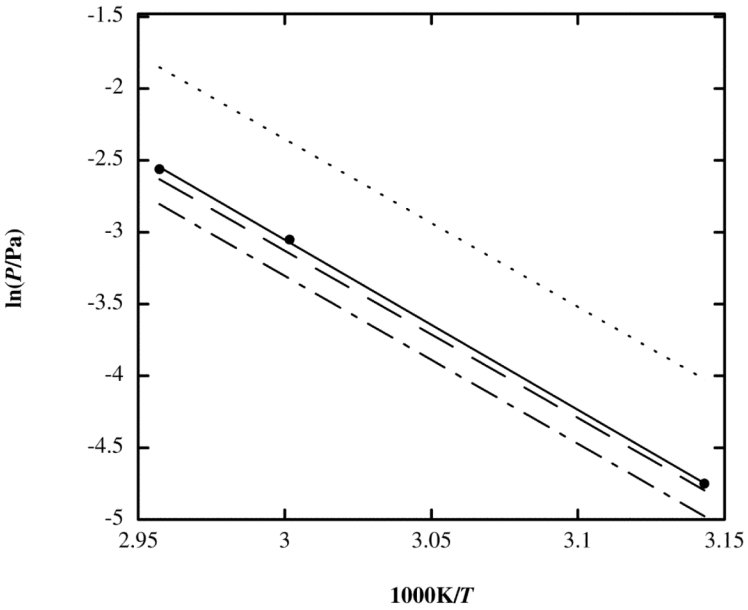

Figure 9.
Vapor pressure of the solid azeotrope at $x_1 = 0.03$: -●-, $P_{measured}$; …, P_{max}; _ _ _, P of azeotrope at $x_1 = 0.14$; _._._, P_2.

Table 1

Melting temperatures of previously reported binary, organic component mixtures that form one eutectic

System	$T_{fus,1}$/K	$T_{fus,2}$/K	$x_{1,e}$	$T_{fus,e}$/K
naphthalene (1) + α-naphthylamine (2)[1]	353.5	323.2	0.36	301.3
naphthalene (1) + α-naphthol (2)[1]	353.5	368.2	0.487	327.7
naphthalene(1) + phenanthrene(2)[1, 2]	353.5	373.2	0.558	321.3
naphthalene (1) + thianaphthene (2)[3, 4]	353.5	305.2	0.063	302.4
naphthalene (1) + diphenyl (2)[3, 4]	353.5	343.7	0.442	312.4
naphthalene (1) + acenaphthene (2)[3, 4]	353.5	368.5	0.564	324.6
naphthalene (1) + fluorene (2)[3, 4]	353.5	388.2	0.613	330.2
naphthalene (1) + fluoranthene (2)[3, 4]	353.5	383.2	0.612	331
Fornaphthalene (1) + pyrene (2)[3, 4]	353.5	423.2	0.746	339.2
naphthalene (1) + chrysene (2)[3, 4]	353.5	528.2	0.971	351.4
biphenyl (1) + fluorene (2)[3, 4]	343.7	388.2	0.909	340.8
biphenyl (1) + acenaphthene (2)[3, 4]	343.7	368.5	0.641	319.3
fluorene (1) + acenaphthene (2)[3, 4]	388.15	368.5	0.431	338.6
phenanthrene (1) + biphenyl (2)[3, 4]	373.2	343.7	0.691	324.8
phenanthrene (1) + acenaphthene (2)[3, 4]	373.2	368.5	0.495	327.5
phenanthrene (1) + pyrene (2)[3, 4]	373.2	423.2	0.747	354.7
anthracene (1) + pyrene (2)[3, 4]	489.8	423.2	0.221	404.6
pyrene (1) + chrysene (2)[3, 4]	423.2	528.2	0.855	405.7
p-dichlorobenzene (1) + p-dibromobenzene (2)[5]	327.2	362.2	0.8325	315.7
resorcinol (1) + p-dibromobenzene (2)[5]	383.2	362.2	0.378	345.95
benzamide (1) + benzoic acid (2)[6]	401.2	395.6	0.5122	356.2
o-chloro benzoic acid (1) + benzoic acid (2)[7]	414.2	394.6	0.3292	368.2

Table 2

Measured melting temperatures and enthalpies of fusion of the anthracene (1) + pyrene (2) system.

x_1	$T_{fus,thaw}$/K	$T_{fus,liquidus}$/K	$\Delta_{fus}H_e$/ J·g^{-1}	$\Delta_{fus}H_{tot}$/ J·g^{-1}
0.00 ± 0	424 ± 1	424 ± 1	0 ± 0	80 ± 5.6
0.10 ± 1·10^{-4}	404 ± 1	419 ± 1	47 ± 3.3	83 ± 5.8
0.12 ± 1·10^{-4}	404 ± 1	418 ± 1	73 ± 5.1	73 ± 5.1
0.15 ± 2·10^{-4}	404 ± 1	415 ± 1	83 ± 5.8	83 ± 5.8
0.18 ± 2·10^{-4}	404 ± 1	413 ± 1	89 ± 6.2	89 ± 6.2
0.20 ± 2·10^{-4}	404 ± 1	409 ± 1	89 ± 6.2	89 ± 6.2
0.22 ± 2·10^{-4}	404 ± 1	406 ± 1	92 ± 6.4	92 ± 6.4
0.24 ± 2·10^{-4}	404 ± 1	409 ± 1	88 ± 6.1	88 ± 6.2
0.26 ± 3·10^{-4}	404 ± 1	413 ± 1	87 ± 6.1	87 ± 6.1
0.28 ± 3·10^{-4}	404 ± 1	418 ± 1	82 ± 5.7	82 ± 5.7
0.30 ± 3·10^{-4}	404 ± 1	422 ± 1	86 ± 6.0	86 ± 6.0
0.50 ± 5·10^{-4}	404 ± 1	453 ± 1	54 ± 3.8	98 ± 6.8
0.75 ± 8·10^{-4}	404 ± 1	475 ± 1	21 ± 1.5	101 ± 7.1
0.90 ± 9·10^{-4}	404 ± 1	485 ± 1	9 ± 0.6	106 ± 7.4
1.00 ± 0	490 ± 1	490 ± 1	0 ± 0	156 ± 10.9

Table 3

Measured vapor pressures of the three solid anthracene (1) + pyrene (2) azeotropes.

Azeotrope x_1 = 0.03		**Azeotrope x_1 = 0.14**		**Azeotrope x_1 = 0.99**	
T/K	*P*/Pa	*T*/K	*P*/Pa	*T*/K	*P*/Pa
318.1	0.0087	318.1	0.00823	307.2	0.0028
333.1	0.0474	333.1	0.04394	309.2	0.0036
338.1	0.0773	338.1	0.07093	311.2	0.0043
				313.2	0.0056
				315.1	0.0071
				317.1	0.0090
				319.2	0.0113
				321.2	0.0143
				323.2	0.0177
				325.2	0.0219
				327.1	0.0273
				333.1	0.0578
				338.1	0.0898